



UvA-DARE (Digital Academic Repository)

Rational Redesign of a Regioselective Hydroformylation Catalyst for 3-Butenoic Acid by Supramolecular Substrate Orientation

Bai, S.-T.; Sinha, V.; Kluwer, A.M.; Linnebank, P.R.; Abiri, Z.; de Bruin, B.; Reek, J.N.H.

DOI

[10.1002/cctc.201900487](https://doi.org/10.1002/cctc.201900487)

Publication date

2019

Document Version

Final published version

Published in

ChemCatChem

License

CC BY-NC

[Link to publication](#)

Citation for published version (APA):

Bai, S-T., Sinha, V., Kluwer, A. M., Linnebank, P. R., Abiri, Z., de Bruin, B., & Reek, J. N. H. (2019). Rational Redesign of a Regioselective Hydroformylation Catalyst for 3-Butenoic Acid by Supramolecular Substrate Orientation. *ChemCatChem*, 11(21), 5322-5329. <https://doi.org/10.1002/cctc.201900487>

General rights

It is not permitted to download or to forward/distribute the text or part of it without the consent of the author(s) and/or copyright holder(s), other than for strictly personal, individual use, unless the work is under an open content license (like Creative Commons).

Disclaimer/Complaints regulations

If you believe that digital publication of certain material infringes any of your rights or (privacy) interests, please let the Library know, stating your reasons. In case of a legitimate complaint, the Library will make the material inaccessible and/or remove it from the website. Please Ask the Library: <https://uba.uva.nl/en/contact>, or a letter to: Library of the University of Amsterdam, Secretariat, Singel 425, 1012 WP Amsterdam, The Netherlands. You will be contacted as soon as possible.

UvA-DARE is a service provided by the library of the University of Amsterdam (<https://dare.uva.nl>)



Rational Redesign of a Regioselective Hydroformylation Catalyst for 3-Butenoic Acid by Supramolecular Substrate Orientation

Shao-Tao Bai,^[a] Vivek Sinha,^[a] Alexander M. Kluwer,^[b] Pim R. Linnebank,^[a] Zohar Abiri,^[b] Bas de Bruin,^[a] and Joost N. H. Reek^{*[a, b]}

Rational design of ligands for regioselective transformations is one of the long pursuing targets in the field of transition metal catalysis. In the current contribution, we report OrthoDIMphos (L2), a ligand that was designed for regioselective hydroformylation of 3-butenic acid and its derivatives. The previously reported ParaDIMphos (L1) based hydroformylation catalyst was very selectively producing the linear aldehyde when substrates were bound in its pocket via hydrogen bonding. However, the distance between the binding site and the rhodium center was too large to also address 3-butenic acid and its derivatives. We therefore designed OrthoDIMphos (L2) as new ligand which has a shorter distance between the

DIM-receptor and the catalytic center. The OrthoDIMphos (L2) based catalyst displays high regioselectivity in the hydroformylation of 3-butenic acid and challenging internal alkene analogue (l/b up to 84, TON up to 630), which cannot be achieved with the ParaDIMphos (L1) catalyst. Detailed studies show that the OrthoDIMphos (L2) based catalyst forms a dimeric structure, in which the two ligands coordinate to two different rhodium metals. Substrate binding to the DIM-receptor is required to break up the dimeric structure, and as only the monomeric analogue is a selective catalyst, the outcome of the reaction is dependent on substrate concentration used in catalysis.

Introduction


Regioselective hydroformylation provides an efficient and 100% atom economical process for the introduction of formyl group to double bonds, and as such it represents one of the key transformations for the pharmaceutical, agrochemical and fragrance industries.^[1] Control over the regioselectivity in this reaction can be challenging and cannot always be achieved by ligand optimization. As such, new concepts and methodologies to control these selectivity issues using alternative strategies are important and received considerable attention.^[1,2] Traditional strategies for the optimization of catalysts rely on a subtle interplay between the metal and the ligand.^[3] Well known ligand parameters that have been optimized in this context include the ligand bite angle, and steric and electronic proper-


ties of the ligand.^[1d,3] In the search for complementary strategies to control difficult selectivity issues, enzymes, nature's catalysts, are often used as a source of inspiration. Enzymes bind substrate molecules in a precise manner with respect to the catalytically active center, leading to exceptionally high selectivity for many different transformations. As a result of the requirement of precise orientation, enzymes often have a limited substrate scope and mutations are required to optimize the system for different substrates. Inspired by this, catalyst design using functional groups for substrate preorganization at transition metal complexes has recently been explored and found to lead to unusually high selectivity for some reactions.^[2d,4,5] In analogy to enzymes, most of these catalysts that rely on substrate orientation have a narrow substrate scope, and as a result such catalysts should be redesigned to extend the substrate scope. Recently, we showcased the first example of the optimization of an active and enantioselective hydrogenation catalyst by strengthening the hydrogen bonding interactions between the substrates and the catalyst.^[6] Catalysts that use hydrogen bonding for substrate orientation^[5,7,12] are known for several reactions, however, the rational redesign of a catalyst based on existing scaffold to widen the substrate scope has to the best of our knowledge not yet been reported, and is the central research question of this paper.


In order to study how such a catalyst can be properly redesigned, we looked at our previously reported ParaDIMphos (L1) catalyst for linear selective hydroformylation using substrate preorganization by supramolecular interactions with the fused DIM-receptor (an anion receptor, Figure 1).^[7] This selective catalyst for ω -unsaturated carboxylic acids, however, cannot convert substrates of which the distance between the carbox-

[a] S.-T. Bai, V. Sinha, P. R. Linnebank, Prof. Dr. B. de Bruin, Prof. Dr. J. N. H. Reek
Supramolecular and Homogeneous Catalysis Group
Van't Hoff Institute for Molecular Sciences (HIMS)
University of Amsterdam
Science Park 904, 1098 XH, Amsterdam (The Netherlands)
E-mail: j.n.h.reek@uva.nl

[b] Dr. A. M. Kluwer, Z. Abiri, Prof. Dr. J. N. H. Reek
InCatT bv., Science Park 904, 1098 XH, Amsterdam (The Netherlands)

 Supporting information for this article is available on the WWW under <https://doi.org/10.1002/cctc.201900487>

 This manuscript is part of the Special Issue on New Concepts in Homogeneous Catalysis.

 © 2019 The Authors. Published by Wiley-VCH Verlag GmbH & Co. KGaA. This is an open access article under the terms of the Creative Commons Attribution Non-Commercial License, which permits use, distribution and reproduction in any medium, provided the original work is properly cited and is not used for commercial purposes.

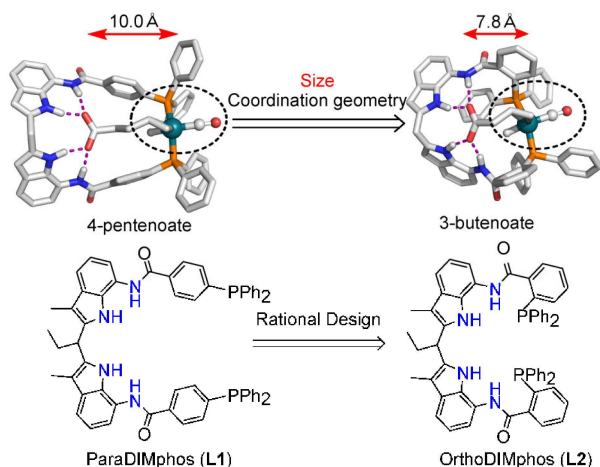


Figure 1. Rational design of OrthoDIMphos (L2) for regioselective hydroformylation of 3-butenic acid via substrate preorganization by changing the distance between the Rh-center and the DIM pocket.

ylate group and the alkene is too short, i.e. 3-butenic acid (l/b 2.6), representing a limitation in substrate scope.^[7b] Regioselective hydroformylation of 3-butenic acid and its internal analogues would be interesting, especially in the context of bio-renewable feedstock conversion, i.e. the production of glutaric acid to make polymers,^[8] or generating 1,5-pentandiol used as plasticizer in cellulose products.^[9] Therefore, we set out to redesign a new catalyst for such regioselective hydroformylation. Molecular modelling studies show that the OrthoDIMphos (L2) based catalyst, a regio-isomer of the ParaDIMphos (L1) analogue, has the proper distance between the binding site and the rhodium center such that it can precisely bind 3-butenate (7.8 Å) (Figure 1). Catalytic experiments show that under the proper conditions the OrthoDIMphos (L2) catalyst displays the highest regioselectivity in the hydroformylation 3-butenic acid reported to date (l/b up to 84), showcasing that this class of supramolecular catalysts are amendable to redesign to widen the substrate scope.

Results and Discussion

The design of the new catalyst is based on DFT calculations of the OrthoDIMphos (L2) and the rhodium complexes thereof. As the hydride migration step generally determines the selectivity, the two monomeric $\text{HRh}(\text{CO})_2(\text{L2})$ -complexes with 3-butenate coordinated to them were calculated, with the hydride pointing in two opposite directions (Figure 2). DFT calculations show that the desired monomeric Rh-complex (A), with the hydride pointing towards the DIM-receptor, is 9.4 kcal mol⁻¹ more stable than the complex (B) with the opposite geometry, in line with what we also found for the analogues complexes based on ParaDIMphos (L1). From intermediate A, hydride migration leads to the catalytic cycle that produces the linear aldehyde, and as such it is predicted that the OrthoDIMphos (L2) based catalyst will hydroformylate 3-butenate in high l/b selectivity.

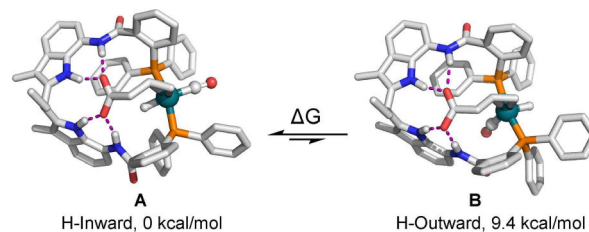


Figure 2. DFT calculations of two monomeric rhodium species that have the hydride pointing towards the DIM-receptor (A) or away from the DIM-receptor (B) (gas phase, BP86-D3/def2-SV(P)//B3LYP-D3/def2-TZVP, Gibbs Free Energy at 298 K).

We next performed HP NMR and IR spectroscopic experiments to identify the rhodium complex formed under hydroformylation conditions. Interestingly, HP NMR and IR spectroscopy of a solution containing a 1:1 mixture of OrthoDIMphos (L2) and $[\text{Rh}(\text{acac})(\text{CO})_2]$ (acac = acetylacetonate) under hydroformylation conditions show that the dimeric complex is the major species, and the monomeric species is only present in small amounts (less than 10%) (Figure 3, Figure S1–10, detailed characterization of the dimeric and monomeric species published in another paper).^[10] Importantly, HP NMR and molecular

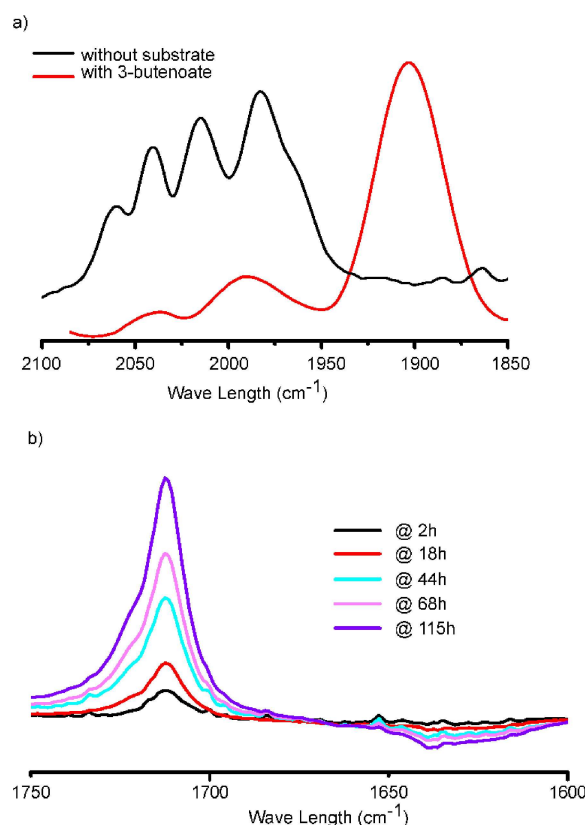


Figure 3. a) HP IR spectroscopy of the dimeric Rh-species (black) and the monomeric species in the presence of 3-butenate (red) under 20 bar of H₂/CO; b) In situ HP IR spectroscopy showing the disappearance of the alkene (1640 cm⁻¹) and formation of the aldehyde (1717 cm⁻¹) in the hydroformylation of 3-butenate.

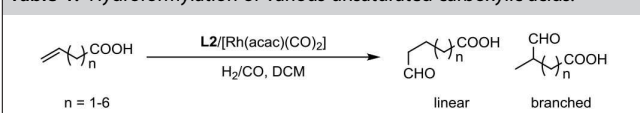
modelling confirm that internal hydrogen bonds are formed between the carbonyl group of one ligand and the DIM-receptor of the dimeric structure. In line with this, HP ^1H NMR also shows inequivalent down field shifts of the protons of the DIM-receptor (1:2:1 ratio, Figure S4–5), further confirming the formation of internal hydrogen bonds. From the modelled structures, it is also clear that in these dimeric structures, the substrate cannot simultaneously bind to the DIM-receptor and the metal center. In contrast, the DIM-receptor of the monomeric Rh-species is free to bind a carboxylate, as evidenced by HP NMR and molecular modelling (Figure S6, 10). As binding of carboxylate groups is strong, substrates containing such functional groups can compete with internal hydrogen bonds and bind to the DIM-receptor, resulting in the formation of the monomeric species at the expense of the dimer. This is also supported by small energy difference calculated between the dimer and the monomer (Figure S10).

We next investigated the structures formed in the presence of substrate under hydroformylation conditions (Figure 3, S8–9). When 160 equivalents of 3-butenolate are present, the *in situ* HP IR spectra shows the formation of a new Rh-complex that shows one broad band in the IR spectrum (1902 cm^{-1} , and two small bands 2044 cm^{-1} and 1991 cm^{-1}),^[11] at the expense of the four bands that are attributed to the dimeric Rh-complex. In contrast, in a similar experiment but in the presence of 160 equivalents of styrene, the four IR bands of the dimer species do not disappear. Importantly, high regioselectivity (l/b 15) was obtained in the presence of 3-butenolate, further suggesting that the monomeric Rh-active species is indeed formed when the carboxylate containing substrate binds to the DIM-receptor.

We next evaluated the OrthoDIMphos (L2) rhodium complex as catalyst in the hydroformylation of a series of (deprotonated) ω -unsaturated carboxylic acids with a range of aliphatic chain lengths between the carboxylic group and the double bond; i.e. from 3-butenic acid to 8-nonenic acid. The neutral acids, i.e. in the absence of base, do not bind to the DIM-receptor, and these conditions were used as control experiments. The linear/branched (l/b) selectivity and aldehyde yield, determined by ^1H NMR spectroscopy, are shown in Table 1 (for details see supporting information).^[12] 3-Butenolate, which is the anionic substrate that precisely spans the distance between the DIM-receptor and the rhodium center of the monomeric active species, was hydroformylated with decent regioselectivity (l/b 8.8, Table 1, entry 1). In contrast, 3-butenic acid (in absence of base) does not bind to the DIM-receptor and was hydroformylated with lower selectivity (l/b 1.6, Table 1, entry 2). Besides the high selectivity achieved via substrate preorganization, the yield is also much higher when the substrate binds to the DIM-receptor (yield of 95% vs. 35%). In line with previous work, this result suggests that the reaction barrier for the formation of the linear aldehyde is lowered and that the local substrate concentration is higher when the substrate binds to the DIM-receptor.

The substrates that are longer than 3-butenolate, from 4-pentenolate to 8-nonenolate, do not show high selectivity for the linear aldehyde when pre-organized in the DIM-receptor of the catalyst, in line with the anticipated narrow substrate scope.

Table 1. Hydroformylation of various unsaturated carboxylic acids.^[a]



Entry	Substrate	Base	l/b	Yield [%]
1	3-butenic acid	yes	8.8	95
2	3-butenic acid	no	1.6	35
3	4-pentenic acid	yes	1.8	87
4	4-pentenic acid	no	2.3	23
5	5-hexenoic acid	yes	1.3	84
6	5-hexenoic acid	no	1.2	90
7	6-heptenoic acid	yes	1.3	81
8	6-heptenoic acid	no	1.4	94
9	7-octenoic acid	yes	1.5	84
10	7-octenoic acid	no	2.3	81
11	8-nonenic acid	yes	1.6	83
12	8-nonenic acid	no	2.4	82

[a] Conditions: $[\text{Rh}(\text{acac})(\text{CO})_2]/\text{OrthoDIMPhos}(\text{L2}) = 1/1.1$, $[\text{Rh}] = 1\text{ mM}$, substrate/Rh 200, 1.0 eq. diisopropylethylamine (DIPEA) or triethylamine (TEA) as the base with respect to the substrate (for uneven entries), 1 ml dichloromethane as the solvent, 40 bar syngas, 40°C , reaction time of 96 hours. No side reactions (isomerization, hydrogenation, etc.) were observed. 1,3,5-Trimethoxybenzene as the internal standard. Conversion and selectivity were determined by ^1H NMR analysis (for 3-butenic acid and 4-pentenic acid, adding 100 μL DIPEA or TEA for NMR analysis). All the catalytic reactions were performed at least in duplo.

In fact, for most of these longer substrates the regioselectivity for the linear aldehyde slightly drops as a result of substrate pre-organization (in presence of base). For 4-pentenolate, the yield is higher when it is pre-organized by binding to the DIM-receptor (Table 1, entry 3–4, 87% vs. 23%) and the selectivity for the linear aldehyde is lower (l/b ratio 1.8 vs. 2.3, Table 1, entry 3–4), which was not expected.

To further understand the selectivity achieved for 3-butenolate and 4-pentenolate, DFT calculations were performed (Figure 4, Figure S11–13 and Table S4). These calculations show that 3-butenolate substrate binds to the catalyst with its C=C double bond parallel with the Rh–H bond, in line with the geometry of 4-pentenolate binding to ParaDIMphos (L1) based catalyst. Also, the alkene can rotate easily to accept the hydride from Rh towards the transition state for the formation of linear aldehyde. Indeed, the computed transition state barrier (C) is only $+11.6\text{ kcal mol}^{-1}$ (relative to complex A). We also tried to find the transition state for the formation of the branched aldehyde, but there are no transition states found that lead to the branched alkyl in which the carboxylate functional group was still in the binding pocket. In addition, we also performed transition state search from substrate preorganized complex B with the Rh-hydride coordination geometry inverted in comparison to A, i.e. H pointing away from the DIM-receptor. As expected, the computed transition state barrier (E) leading to the branched product is much higher than the barrier from A to D (21.2 vs. $11.6\text{ kcal mol}^{-1}$ relative to complex A). Thus, the branched product is probably formed via a pathway in which the carboxylate group is not bound in the DIM-receptor.

We next performed DFT calculations on 4-pentenolate substrate (Figure S12–13 and Table S4). In contrast to 3-butenolate, 4-pentenolate binds ditopically to the Rh(L2)-catalyst

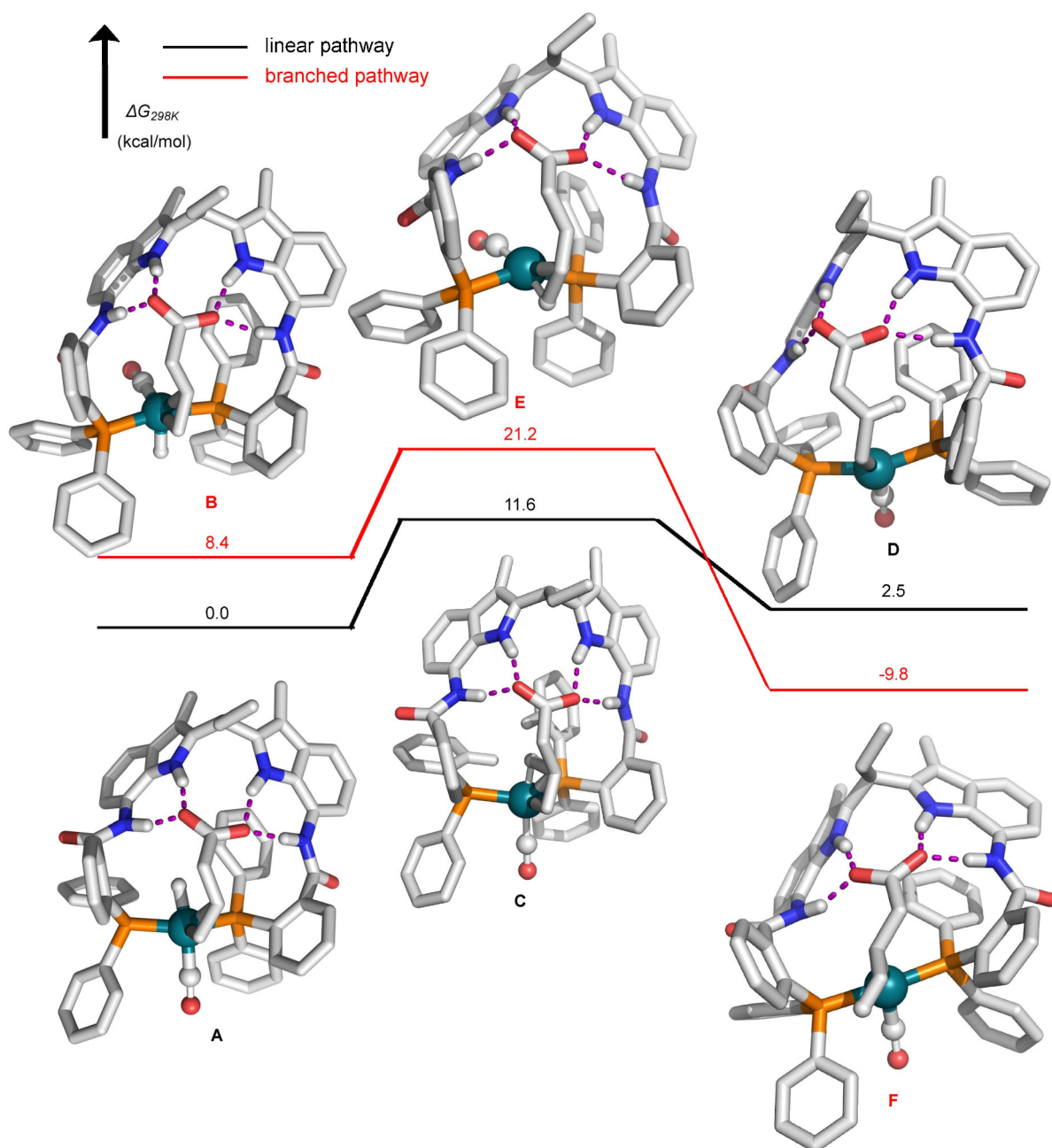


Figure 4. DFT calculated hydride migration steps, crucial for the selectivity in the hydroformylation of 3-butenolate (BP86-D3/def2-SV(P)//B3LYP-D3/def2-TZVP/COSMO(DCM)).

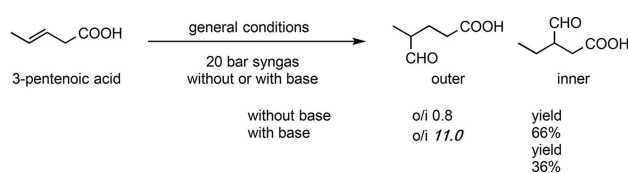
with C=C double bond perpendicular to Rh–H bond for both complexes with hydride pointing in opposite directions. In these geometries, both carbon atoms of the C=C double are accessible for hydride migration, leading to the formation of both linear and branched Rh-alkyl species. The difference in transition state energy between the pathways that lead to the linear and branched Rh-alkyl species is around 2.0 kcal mol⁻¹ (19.4 vs. 21.4 kcal mol⁻¹, Figure S12–13, Table S4), in line with the observed trend in the experiment. Furthermore, single point calculations on substrate taken from the transition states show that the substrate has to fold during hydride formation that

results in linear aldehyde formation, which is energetically unfavorable, explaining the slightly lower selectivity as a result of substrate pre-organization. Importantly, in line with experimental observations, DFT calculations show that the substrate that is one carbon atom longer (4-pentenoate vs. 3-butenolate) can be pre-organized by this catalyst, but this does not lead to selective hydroformylation.

Hydroformylation of longer substrates, ranging from 5-hexenoic acid to 8-nonenoic acid, shows a similar pattern, i.e. the regioselectivity slightly shifts in favor of the branched product when the anionic substrates bind to the DIM-receptor

(Table 1, entry 5–12). Note that in these reactions the absence/presence of base has little influence on the yield, thus indicating that pre-organization of the substrate to the catalyst doesn't change the activity (Table 1, entry 5–12). In comparison, the ParaDIMPhos (L1) based catalyst^[7] displays high linear selectivity (l/b 20–50) for all these longer substrates, from 4-pentenoate to 8-nonenoate, showing that the substrate scope of the new ligand is narrow. Similar findings were reported by Breit et al., who reported a monodentate ligand in which the binding site is also close to the metal center, and also in that case the substrate scope is narrow.^[12]

We further extended the scope to internal alkene substrates, which are challenging substrates in rhodium catalyzed hydroformylation because of lower reactivity and internal alkenes are generally converted with low regioselectivity as the carbon atoms of the double bond are very similar (Scheme 1).^[1f,13] We



Scheme 1. Hydroformylation of 3-pentenoic acid. Conditions: [Rh(acac)(CO)₂]/OrthoDIMPhos(L2) = 1/1.1, [Rh] = 1 mM, substrate/Rh 200, 1.0 eq. diisopropylethylamine (DIPEA) or triethylamine (TEA) as the base with respect to the substrate (in case base is used), 1 ml dichloromethane as the solvent, 20 bar syngas, 40 °C, reaction time of 96 hrs. 3-Pentenoic acid is mainly *trans*-form with 5–6% *cis*-isomer obtained from Sigma-Aldrich. No side reactions (isomerization, hydrogenation, etc.) were observed. 1,3,5-Trimethoxybenzene as the internal standard. Conversion and selectivity were determined by ¹H NMR analysis (adding 100 uL DIPEA or TEA for NMR analysis). All the catalytic reactions were performed at least two runs.

explored the conversion of 3-pentenoate, which precisely spans the distance between the DIM-receptor and the rhodium center, just like 3-butenate. Gratifyingly, the substrate was hydroformylated with high regioselectivity in the presence of base via substrate pre-organization (o/i 11.0, Scheme 1). In the control experiment, in the absence of base, 3-pentenoic acid was converted to an almost 1:1 mixture of the two aldehydes as could be expected (o/i 0.8, Scheme 1). Interestingly, the yield reduced from 66% to 36% when 3-pentenoate binds to the DIM-receptor due to the generally higher activity displayed by the dimer species which is not compensated for by substrate pre-organization for this substrate.^[10g]

In order to investigate the properties of the dimeric and monomeric catalytic species in the hydroformylation of 3-butenate, we performed reaction kinetic studies monitored by gas-uptake experiments under standard conditions. The reaction rate and selectivity dependence on the rhodium concentration (0.2–3.2 mM) was investigated at substrate concentration of 0.6 M (Figure 5. Table S2 and Figure S14–16). Importantly, as substrate binding to the DIM-receptor is the driving force to form monomeric species, we expected to observe an unusual reaction order in rhodium. We observed a linear dependency of the reaction rate on the rhodium

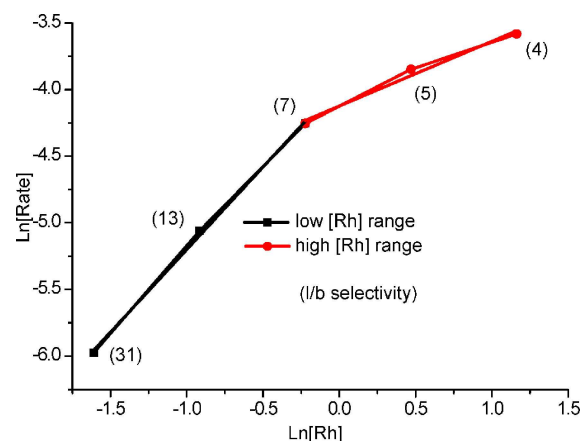


Figure 5. Reaction rate and regioselectivity (given in brackets) vs rhodium concentration. Reaction conditions: the rhodium concentration was varied between 0.2 mM and 3.2 mM at substrate concentration of 0.6 M, solvent dichloromethane, total volume 9 mL, pressure 40 bar, reaction temperature 40 °C, stirring speed 800 rpm

concentration in the lower concentration range (0.2–0.8 mM), suggesting that the monomeric Rh-complex is the dominant species at low rhodium concentration. In contrast, in the higher concentration range, the reaction order in rhodium is around 0.5 (0.8–3.2 mM), suggesting that mainly dimeric complexes are present. If this dimer is broken in the rate determining step, a half order is expected. Also, the selectivity is higher at lower rhodium concentration (l/b 4–31, Figure 5 and Table S2), indicating that the monomeric Rh-complex becomes more dominant in catalysis. At high rhodium concentration the dimeric complex is the dominant species, and some of the substrate is also converted by the dimer, and as in this complex the substrate cannot ditopically bind, this results in lower selectivity for the linear aldehyde.

Next, the reaction rate and selectivity dependency on the substrate concentration (0.1–1.6 M) was investigated at a rhodium concentration of 0.8 mM (Figure 6 a–b, Table S2 and Figure S17–19). We converted the conversion plots into rate/substrate concentration plots, as reaction progress kinetic analysis (RPKA)^[14] curves of 0.4, 0.8 and 1.6 M substrate concentration provide extra information. As these lines do not overlap, we can conclude that the reaction follows a kinetic profile that also includes inhibition process, which was previously also observed for complexes based on ParaDIMPhos (L1)^[7,15] (Figure 6. a and Figure S18). From the gas uptake curves, we also calculated the rate from the slope at the start of the reaction, and plotted these rates as function of the substrate concentration. As is clear, in the window of 0–0.4 M, the rate increases with the substrate concentration, but above this concentration the rate drops again. This suggests that at these high substrate concentrations (0.4 M–1.6 M) substrate inhibition plays a role, a phenomenon that was previously also observed for rhodium catalysts based on phosphite DIMPhos ligands, likely because dormant state species are formed via carboxylate coordination to Rh metal.^[11c] Importantly, higher selectivity for the linear aldehyde was observed at higher substrate concen-

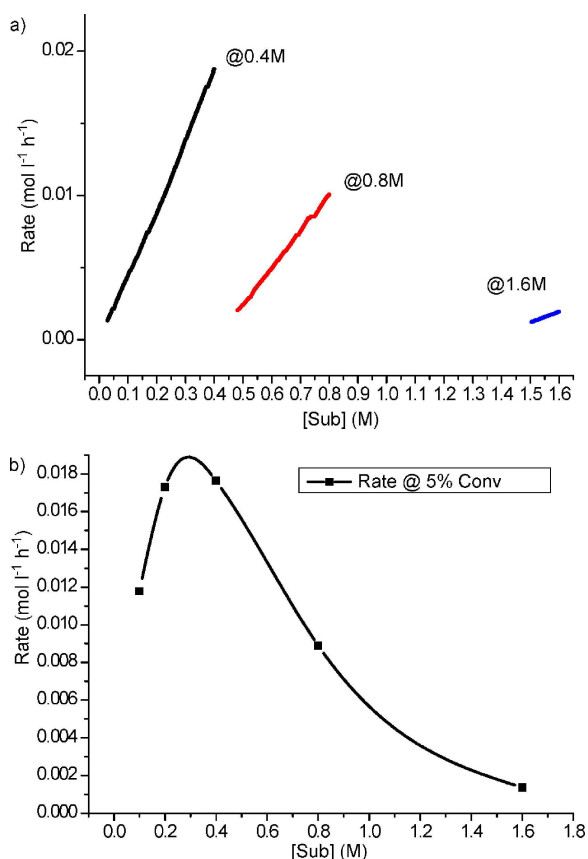


Figure 6. a). Reaction Progress Kinetic Analysis (RPKA) curves constructed from the recorded gas-uptake curves (the RPKA plot displays the rate as function of the substrate concentration). b). Reaction rate determined at 5% conversion vs. substrate concentration. Reaction conditions: the substrate concentration was varied between 0.1 M and 1.6 M at rhodium concentration of 0.8 mM, solvent dichloromethane, total volume 8 mL, pressure 40 bar, reaction temperature 40 °C, stirring speed 800 rpm.

tration (Table S2). With this information at hand we further optimized the conditions to achieve higher selectivity in the hydroformylation of 3-butenic acid, and we performed some additional control experiments (Table 2). When increasing the ratio of carboxylate/DIM-receptor, the selectivity was improved

Table 2. Optimization of catalysis conditions and control experiments for regioselective hydroformylation of 3-butenic acid.

Entry	Substrate	additives	Sub/Rh	l/b	Yield [%] (TON)
1 ^[a]	3-butenic acid	no	200	1.6	35(70)
2 ^[a]	3-butenic acid	200 TEA	200	8.8	95(190)
3 ^[b]	3-butenic acid	600 TEA	600	19	37(222)
4 ^[c]	3-butenic acid	3000 TEA	3000	84	21(630)
5 ^[a]	3-butenic acid	3000 TEA-Acetic acid	200	16	8(-)
6 ^[a]	3-butenic acid	no	3000	1.6	3(-)

[a] Conditions: [Rh(acac)(CO)₂]/OrthoDIMPhos(L2) = 1/1.1, [Rh] = 1 mM, 1 ml dichloromethane as the solvent, 40 bar syngas, 40 °C, reaction time of 96 hours. 1,3,5-Trimethoxybenzene as the internal standard. Conversion and selectivity were determined by ¹H NMR analysis (adding 100 µL DIPEA or TEA for NMR analysis). [b] [Rh] = 0.6 mM. [c] [Rh] = 0.2 mM.

from 8.8 to 19 and 84 at substrate/rhodium ratio of 200, 600 and 3000, respectively, and also the TON increased from 190 to 630 (Table 2 entry 1–4). As noted previously, in the absence of base the higher selectivity is lost (Table 2 entry 1, 5, l/b 1.6 vs 8.8). Also, at high substrate loading but in the absence of base the selectivity is low (l/b 1.6, Table 2 entry 6), as neutral acids cannot bind to the DIM-receptor. These results combined with in situ spectroscopy studies, DFT calculations and kinetic experiments confirm that substrate binding to the DIM-receptor is the driving force converting the dimeric to monomeric species, which allows linear selective hydroformylation by substrate preorganization.

Conclusions

Enzymes enable very selective chemical conversions; however, they generally display a rather narrow substrate scope. As such, when using enzymes for synthetic applications re-engineering of the enzyme may be required to adapt it for new substrates. We previously reported a catalyst that controls the selectivity by substrate orientation, reminiscent of enzymes, which was based on ParaDIMphos (L1). Carboxylate containing alkene substrates were pre-organized at the metal center via the DIM-binding pocket, resulting in linear selective hydroformylation. The distance between the binding pocket and the rhodium complex was, however, too long to also selectively convert 3-butenic acid. To widen the substrate scope, we redesigned the ligand for regioselective hydroformylation of these type of shorter substrates, which resulted in the development of a new ligand coined OrthoDIMphos (L2). DFT calculations show that the OrthoDIMphos (L2) based rhodium catalyst has a shorter distance between the DIM-receptor and the Rh center, such that 3-butenic acid can bind simultaneously to the rhodium center (with the alkene) and the binding pocket (with the acetate). Indeed, under optimized conditions the OrthoDIMphos (L2) based catalyst displays the highest regioselectivity in the hydroformylation of 3-butenic acid reported to date (l/b up to 84, TON up to 630). The internal alkene analogue, 3-pentenoate, was also converted with high regioselectivity (o/i = 11). This catalyst cannot convert longer substrates with high regioselectivity. In this paper we demonstrate that we can redesign a catalyst that operates via supramolecular substrate orientation in order to adapt it for others substrates. As supramolecular substrate orientation is an increasingly popular strategy to achieve selectivity in catalysis, this redesign of such catalysts may stimulate other to follow similar approaches in widening the substrate scope.

Experimental Section

A catalyst stock solution for the hydroformylation experiments was prepared by charging a flame-dried Schlenk flask with Rh(acac)(CO)₂, ligand, *N,N*-diisopropylethylamine (DIPEA) or triethylamine (TEA), if appropriate, internal standard (1,3,5-trimethoxybenzene) and dried and degassed dichloromethane with standard Schlenk technique or in the Glove-Box. The solution was stirred for 30

minutes and then 1.5 mL reaction vials (pre-dried in oven overnight) equipped with mini-Teflon stirring bars were charged with the appropriate amount of substrates followed by the addition of proper amount of catalyst stock solution in the Glove-Box. The vials were placed in a stainless steel autoclave (250 mL) charged with an insert suitable for 8 reaction vials for conducting parallel reactions. The autoclave was closed properly and then purged three times with 30 of bar syngas followed by pressurized at 40 or 20 bar of syngas. The reaction mixtures were stirred under appropriate temperature for the required reaction time, after which the pressure was released and the yield and regioselectivity were determined by ^1H NMR analysis with 200 scans to reduce the baseline effects. For NMR analysis, usually 100 μL reaction mixture were evaporated under reduced pressure followed by adding proper amount of CDCl_3 (for 3-butenic acid and 4-pentenoic acid, 50 μL DIPEA or TEA was added into the NMR tube otherwise the branched aldehyde cannot be resolved). Analysis of characteristic signals in the aliphatic and aldehyde regions were in agreement in all cases.

All DFT calculations were performed with the Turbomole program coupled to the PQS Baker optimizer via the BOpt package. Geometries were fully optimized as minima using the BP86 functional and the resolution-of-identity (ri) method using the Turbomole def2-SVP basis for all atoms. On the optimized geometries, single-point energy calculations were carried out using the B3LYP functional in conjunction with a triple-zeta quality def2-TZVP basis set to obtain more accurate reaction energies. Grimme's dispersion corrections (D3 version, implemented with the keyword disp3 in Turbomole) were applied in all calculations. Solvent effects (COSMO) were included in the calculation of the crucial hydride-migration steps in the hydroformylation of the 4-pentenoate and 3-butenate anion. All minima (no imaginary frequencies) were characterized by calculating the Hessian matrix. ZPE and gas-phase thermal corrections (entropy and enthalpy, 298 K, 1 bar) from these analyses were calculated. The relative free and enthalpies obtained from these calculations are reported in the main text of this paper.

Acknowledgements

S.-T. Bai thanks the China Scholarship Council for a PhD fellowship (CSC student number 201506010269) and University of Amsterdam for financial support. VS and BdB thank the NWO-Shell Computational sciences for energy research initiative (project 13CSER003) and the RPA Sustainable Chemistry of the University of Amsterdam, and PRL and JNHR thank NWO and InCatV bv. for financial Support.

Conflict of Interest

The authors declare no conflict of interest.

Keywords: rational catalyst design · substrate preorganization · rhodium catalyzed hydroformylation · supramolecular catalysis

[1] For books and reviews see: a) B. Cornils, W. A. Herrmann, C. D. Frohning, C. W. Kohlpaintner, H.-W. Bohnen, A. Hohn, M. Beller, J. F. Knifton, A. Klausener, J.-D. Jentsch, *Applied Homogeneous Catalysis with Organometallic Compounds* (Ed.: B. Cornils and W. A. Herrmann), Wiley-VCH

Verlag GmbH, Weinheim, Germany, 2002; b) P. W. N. M. van Leeuwen, *Homogeneous Catalysis: Understanding the Art*, Springer Netherlands, Dordrecht, 2004; c) M. Torrent, M. Solà, G. Frenking, *Chem. Rev.* 2000, 100, 439–494; d) B. Breit, in *Metal Catalyzed Reductive C–C Bond Formation* (Ed.: M. J. Krische), Springer Berlin Heidelberg, Berlin, Heidelberg, Heidelberg, 2007, pp. 139–172; e) J. G. de Vries, in *C-1 Build. Blocks Org. Synth. 1* (Ed.: P. W. N. M. van Leeuwen), Georg Thieme Verlag, Stuttgart, 2014, pp. 193–227; f) R. Franke, D. Selent, A. Börner, *Chem. Rev.* 2012, 112, 5675–5732; g) P. C. J. Kamer, J. N. H. Reek, P. W. N. M. van Leeuwen, R. Lazzaroni, R. Settambolo, A. Caiazzo, C. P. Casey, G. T. Whiteker, C. Claver, S. Castillón, *Rhodium Catalyzed Hydroformylation* (Ed.: W. N. M. van Leeuwen and C. Claver), Wiley-VCH Verlag GmbH & Co. KGaA, Weinheim, FRG, 2005.

- [2] For reviews see: a) M.-N. Birkholz, Z. Freixa, P. W. N. M. van Leeuwen, *Chem. Soc. Rev.* 2009, 38, 1099–1118; b) P. W. N. M. van Leeuwen, P. C. J. Kamer, J. N. H. Reek, P. Dierkes, *Chem. Rev.* 2000, 100, 2741–2769; c) R. F. Heck, *Acc. Chem. Res.* 1979, 12, 146–151; d) B. Zhao, Z. Han, K. Ding, *Angew. Chem. Int. Ed.* 2013, 52, 4744–4788; e) D. Benito-Garagorri, K. Kirchner, *Acc. Chem. Res.* 2008, 41, 201–213; f) P. C. J. Kamer, P. W. N. M. van Leeuwen, J. N. H. Reek, *Acc. Chem. Res.* 2001, 34, 895–904; g) A. A. Oswald, D. E. Hendriksen, R. V. Kastrup, K. Irikura, E. J. Mozeleski, D. A. Young, *Phosphorus Sulfur Relat. Elem.* 1987, 30, 237–240; h) S. Würtz, F. Glorius, *Acc. Chem. Res.* 2008, 41, 1523–1533; i) C. A. Tolman, *Chem. Rev.* 1977, 77, 313–348; j) H. M. L. Davies, D. Morton, *Chem. Soc. Rev.* 2011, 40, 1857–1857; k) M. L. Clarke, J. J. R. Frew, *Organomet. Chem.* 2009, 35, 19–46; l) J. F. Hartwig, *Chem. Soc. Rev.* 2011, 40, 1992; m) J. F. Hartwig, *Acc. Chem. Res.* 2012, 45, 865–873.
- [3] See review and references cited herein: a) C. Jäkel, R. Paciello, *Chem. Rev.* 2006, 106, 2912–2942; b) M. T. Reetz, *Angew. Chem. Int. Ed.* 2008, 47, 2556–2588; c) B. Breit, *Pure Appl. Chem.* 2008, 80, 855–860; d) P. E. Goudriaan, P. W. N. M. van Leeuwen, M.-N. Birkholz, J. N. H. Reek, *Eur. J. Inorg. Chem.* 2008, 2939–2958.
- [4] For reviews, books and contributions on encapsulated catalysts featured with substrate preorganization, see: a) D. Zhang, A. Martinez, J. P. Dutasta, *Chem. Rev.* 2017, 117, 4900–4942; b) C. J. Brown, F. D. Toste, R. G. Bergman, K. N. Raymond, *Chem. Rev.* 2015, 115, 3012–3035; c) J. A. A. W. Elemans, J. J. L. M. Cornelissen, M. C. Feiters, A. E. Rowan, R. J. M. Nolte, in *Supramolecular Catalysis*, Wiley-VCH Verlag GmbH & Co. KGaA, Weinheim, Germany, 2008, pp. 143–164; d) D. Rix, J. Lacour, *Angew. Chem. Int. Ed.* 2010, 49, 1918–1920; e) S. Carboni, C. Gennari, L. Pignataro, U. Piarulli, *Dalton Trans.* 2011, 40, 4355–4373; f) S. H. A. M. Leenders, R. Gramage-Doria, B. de Bruin, J. N. H. Reek, *Chem. Soc. Rev.* 2015, 44, 433–448; g) A. W. Kleij, J. N. H. Reek, *Chem. Eur. J.* 2006, 12, 4218–4227; h) M. Yoshizawa, J. K. Klosterman, M. Fujita, *Angew. Chem. Int. Ed.* 2009, 48, 3418–3438; i) L. J. Jongkind, X. Caumes, A. P. T. Hartendorp, J. N. H. Reek, *Acc. Chem. Res.* 2018, 51, 2115–2128.
- [5] For reviews on supramolecular substrate orientation, see: a) M. Raynal, P. Ballester, A. Vidal-Ferran, P. W. N. M. van Leeuwen, *Chem. Soc. Rev.* 2014, 43, 1734–1787; b) M. Vaquero, L. Rovira, A. Vidal-Ferran, *Chem. Commun.* 2016, 52, 11038–11051; c) J. Meeuwissen, J. N. H. Reek, *Nat. Chem.* 2010, 2, 615–621; d) P. Dydio, J. N. H. Reek, *Chem. Sci.* 2014, 5, 2135–2145; e) H. J. Davis, R. J. Phipps, *Chem. Sci.* 2017, 8, 864–877; f) S. S. Nurtila, P. R. Linnebank, T. Krachko, J. N. H. Reek, *ACS Catal.* 2018, 8, 3469–3488; g) E. Lindback, S. Dawagheer, K. Warming, *Chem. Eur. J.* 2014, 20, 13532–13481. For contributions on supramolecular substrate orientation. h) S. Das, C. D. Incarvito, R. H. Crabtree, G. W. Brudvig, *Science*, 2006, 312, 1941–1943. i) A. Bauer, F. Westkamper, S. Grimme, T. Bach, *Nature*, 2005, 436, 1139–1140. j) S. C. Coote, T. Bach, *J. Am. Chem. Soc.*, 2013, 135, 14948–14951. k) T. Šmejkal, B. Breit, *Angew. Chem. Int. Ed.* 2008, 47, 3946–3949.
- [6] J. Daubignard, R. J. Detz, A. C. H. Jans, B. de Bruin, J. N. H. Reek, *Angew. Chem. Int. Ed.* 2017, 56, 13056–13060.
- [7] a) P. Dydio, R. J. Detz, J. N. H. Reek, *J. Am. Chem. Soc.* 2013, 135, 10817–10828; b) P. Dydio, W. I. Dzik, M. Lutz, B. de Bruin, J. N. H. Reek, *Angew. Chem. Int. Ed.* 2011, 50, 396–400. c) P. Dydio, J. N. H. Reek, *Angew. Chem. Int. Ed.* 2013, 52, 3878–3882; d) P. Dydio, M. Ploeger, J. N. H. Reek, *ACS Catal.* 2013, 3, 2939–2942; e) P. Dydio, J. N. H. Reek, *Nat. Protoc.* 2014, 9, 1183–1191.
- [8] G. Paris, L. Berlinguet, R. Gaudry, *Org. Synth.* 1957, 37, 47.
- [9] a) P. Werle, M. Morawietz, S. Lundmark, K. Sörensen, E. Karvinen, J. Lehtonen, in *Ullmann's Encyclopedia Industrial Chemistry*, Wiley-VCH Verlag GmbH & Co. KGaA, 2000; b) J. J. Sundberg, J. Faergemann, *Expert Opin. Invest. Drugs* 2008, 17, 601–610.
- [10] For general characterization of the rhodium complexes see: a) S. H. Chikkali, J. I. van der Vlugt, J. N. H. H. Reek, *Coord. Chem. Rev.* 2014, 262,

- 1–15; b) T. Pechmann, C. D. Brandt, H. Werner, *Dalton Trans.* **2004**, 959–966; c) T. H. Brown, P. J. Green, *J. Am. Chem. Soc.* **1970**, *92*, 2359–2362; d) P. E. Kreter, D. W. Meek, *Inorg. Chem.* **1983**, *22*, 319–326; e) T. Pechmann, C. D. Brandt, H. Werner, *Chem. Commun.* **2003**, 1136–1137; f) P. C. J. Kamer, A. van Rooy, G. C. Schoemaker, P. W. N. M. van Leeuwen, *Coord. Chem. Rev.* **2004**, *248*, 2409–2424 For specific characterization of the dimer complex see g) S.-T. Bai, V. Sinha, A. M. Kluwer, P. R Linnebank, Z. Abiri, P. Dydio, M. Lutz, B. de Bruin, J. N. H. Reek, submitted.
- [11] For relevant HP-IR bands observed in literatures see: a) Y. S. Varshavskii, T. G. Cherkasova, I. S. Podkorytov, A. A. Korlyukov, V. N. Khrustalev, A. B. Nikol'skii, *Russ. J. Coord. Chem.* **2005**, *31*, 121–131; b) D. Evans, J. A. Osborn, G. Wilkinson, *J. Chem. Soc. A.* **1968**, *0*, 3133–3142; c) P. Dydio, R. J. Detz, B. de Bruin, J. N. H. Reek, *J. Am. Chem. Soc.* **2014**, *136*, 8418–8429.
- [12] For NMR analysis of the regioselectivity see references: a) T. Šmejkal, D. Gribkov, J. Geier, M. Keller, B. Breit, *Chem. Eur. J.* **2010**, *16*, 2470–2478; b) T. Šmejkal, B. Breit, *Angew. Chem. Int. Ed.* **2008**, *47*, 311–315.
- [13] a) L. A. van der Veen, P. C. J. Kamer, P. W. N. M. van Leeuwen, *Angew. Chem. Int. Ed.* **1999**, *38*, 336–338; b) D. Selent, K.-D. Wiese, D. Röttger, A. Börner, *Angew. Chem. Int. Ed.* **2000**, *39*, 1639–1641.
- [14] See the review and the references cited herein: D. G. Blackmond, *Angew. Chem. Int. Ed.* **2005**, *44*, 4302–4320.
- [15] We previously reported carboxylate containing molecules binding to the ParaDIMphos type catalyst is the main reason observed for inhibition process. In line with that, we also observed similar behavior is observed for this redesigned catalyst that both substrate and product could cause that inhibition. Details see the references of [6].

Manuscript received: March 20, 2019
 Revised manuscript received: April 5, 2019
 Accepted manuscript online: April 8, 2019
 Version of record online: April 30, 2019